Icarus 224 (2013) 209–217

Contents lists available at SciVerse ScienceDirect

Icarus

journal homepage: www.elsevier.com/locate/icarus

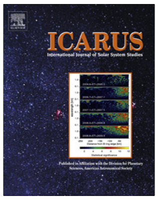

Impact experiments of exotic dust grain capture by highly porous primitive bodies

Takaya Okamoto [a,*], Akiko M. Nakamura [a], Sunao Hasegawa [b], Kosuke Kurosawa [b], Katsutoshi Ikezaki [c], Akira Tsuchiyama [d]

[a] *Department of Earth and Planetary Sciences, Kobe University, 1-1 Rokkodai, Nada-ku, Kobe 657-8501, Japan*
[b] *Institute of Space and Astronautical Science, JAXA, 3-1-1 Yoshinodai, Chuo-ku, Sagamihara, Kanagawa 252-5210, Japan*
[c] *Department of Earth and Space Science, Osaka University, 1-1 Machikaneyama, Toyonaka, Osaka 560-0043, Japan*
[d] *Division of Earth and Planetary Sciences, Kyoto University, Kitashirakawaoiwake-cho, Sakyo-ku, Kyoto 606-8502, Japan*

ARTICLE INFO

Article history:
Received 16 August 2012
Revised 14 February 2013
Accepted 14 February 2013
Available online 6 March 2013

Keywords:
Impact processes
Comets, Origin
Comets, Dust
Planetesimals
Kuiper Belt

ABSTRACT

Small primitive bodies were presumably highly porous when they formed and some still have low densities that are indicative of a high pore content. Therefore, after their formation, interplanetary dust impacting on their surface may have been captured because of their porous structure. The mechanism of dust penetration is thus of importance to understand the evolution of small bodies and the origin of their internal dust particles. Impact experiments of sintered glass-bead targets characterized by 80%, 87%, and 94% bulk porosity were conducted using metal and basalt projectiles at impact velocities ranging from 1.6 to 7.2 km s^{-1}. Track morphology and penetration processes were analyzed using both X-ray tomography and a flash X-ray system. Two types of track were observed, as previously also found in the Stardust aerogel: a thin and long track (carrot-shaped track), and a “bulb” with tails (bulb-shaped track). The track shape changed with initial dynamic pressure. We found that the transition between “carrot” and “bulb” occurred at a pressure of roughly 20 times the projectile’s tensile strength. The deceleration process of projectiles without severe deformation and fragmentation was reproduced by a drag equation composed of an inertia drag that was proportional to the square of the projectile’s velocity and a constant drag proportional to the target’s compressive strength. We applied this deceleration equation to silicate dust penetrating into hypothetical porous icy bodies which were homogeneous on much smaller scales than the impacting dust particles. The penetration depth was approximately 100 times the projectile diameter for the bodies with 90% porosity.

1. Introduction

Early planetesimals that formed from dust aggregates are thought to have been very porous. Numerical simulations of sequential collisions of water–ice dust aggregates showed that aggregates in protoplanetary disks had an extremely low density (<0.1 kg m^{-3}), which corresponds to a bulk porosity of more than 99% (Suyama et al., 2008). The previous experimental study (Blum and Wurm, 2008) also showed that laboratory-grown random ballistic-deposition aggregates of non-ice particles (<1 μm) have been shown to have a bulk porosity of 85% if mono-disperse spherical dust grains are used. Deviation from sphericity resulted in an increase of the porosity to 89%, whereas a wide size distribution of irregularly shaped monomers yielded an even higher porosity of 93%.

Planetesimals collided with each other and evolved into small primitive bodies, and their bulk porosity decreased through mechanisms such as compaction and sintering. However, some of the resulting small bodies—such as asteroids, comets, and Kuiper Belt Objects (KBOs)—still have high bulk porosities. The macroporosities of C-class asteroids, for example, are estimated to range from a few to 60% if asteroids are assumed to consist of carbonaceous chondrites. The macroporosities of comets are estimated to be even higher, up to 86%, if comets are assumed to consist of water ice and organic material with a CM-like density (Consolmagno et al., 2008). Thus, small primitive bodies have been porous throughout the history of the Solar System. Dust can be captured at the surface of such highly porous bodies long after their formation.

Dust particles from Comet 81P/Wild 2, a Jupiter-family comet (JFC) that is believed to have formed in the Kuiper Belt and to have only recently entered the inner regions of the Solar System, were returned to Earth by the Stardust mission (Brownlee et al., 2006). The dust particles were analyzed and found to contain refractory objects resembling meteoritic Calcium–Aluminum-rich Inclusion (CAI) (e.g., Brownlee et al., 2006; McKeegan et al., 2006; Zolensky et al., 2006). Numerous Wild 2 particles also have been shown to be either chondrule fragments or chondrule-like fragments

---

* Corresponding author. Fax: +81 78 803 6483.
E-mail address: tokamoto@stu.kobe-u.ac.jp (T. Okamoto).

0019-1035/$ - see front matter © 2013 Elsevier Inc. All rights reserved.
http://dx.doi.org/10.1016/j.icarus.2013.02.023

(e.g. Nakamura et al., 2008; Ogliore et al., 2012). The presence of high-temperature objects in a comet such as CAI-like, chondrule-like and chondrule fragments suggests that the objects formed near the Sun were transported to the formation region of the icy bodies. In addition, spectroscopic observations of both Oort Cloud and Jupiter-family comets found that comets consist of crystalline silicate materials, which are produced by a high-temperature process (Harker et al., 2005). It is also thought that the crystalline silicates in comets are evidence of active material transport in the radial direction in the protoplanetary disk (Wooden et al., 2007).

There are two possibilities as to when and how during the history of the Solar System the refractory grains became components of the small icy bodies. The first assumes that the grains were original components of these bodies during the accretion stage, and that they were somehow transported from the inner part of the nebula and then mixed with the initial dust component of the formation region of the icy planetesimals. The second possibility is that grains were collected in a debris disk after the bodies formed. In the second process, exotic components would have accumulated on the surface of the icy bodies and changed their surface composition. For example, short-period comet nuclei would accumulate meteoroids as a consequence of collisions with asteroidal debris (Cintala, 1981).

The purpose of this study is to investigate the penetration depth of dust into small porous bodies. Dust penetration into silica aerogel has been studied extensively for calibration of the Stardust tracks (e.g., Niimi et al., 2011). However, it is not clear how far the understanding thus gained can be extrapolated to dust penetration into small porous primitive bodies in a planetary system. Laboratory impact experiments of cratering and disruption processes of porous targets have been conducted and scaling laws have been studied (Love et al., 1993; Housen and Holsapple, 2003; Setoh et al., 2010; Yasui et al., 2012). In this study, we focus on the penetration process of projectiles into highly porous targets to gain a better understanding of the physical processes of dust penetration into small porous bodies. We conducted impact-penetration experiments of millimeter-sized metal and rock projectiles into highly porous sintered targets, which consisted of pores that were much smaller than the projectiles themselves. Yasui et al. (2012) performed similar experiments of a gypsum target with bulk porosity of 50% using metal and nylon projectiles for observation of crater formation and projectile penetration. Targets in this study were much porous with bulk porosities up to 94%. We investigated the deceleration process as well as deformation and fragmentation degree of the projectiles in the porous bodies.

2. Experiments

We prepared sintered targets characterized by three bulk porosities using glass beads. The preparation procedure was similar to that used in previous experiments (Setoh et al., 2010; Machii and Nakamura, 2011). The sintering conditions and the physical properties of the individual targets are listed in Table 1. Hollow soda–lime–borosilicate glass microspheres (3M Co.), with an average diameter and shell thickness of 55 μm, 0.95 μm, respectively, isostatic crush strength of 5.2 MPa and a grain density of 2.5 g cm^{-3}, were sintered in a cylindrical mold of 67 mm in inner diameter, 150 mm in inner height and 10 mm in thickness with a lid of 5 mm in thickness. The targets were heated for 6 h to two different peak temperatures to attain bulk porosities of 87% and 94%. Low-alkali glass particles of 5 μm in diameter (on average) and 2.6 g cm^{-3} in grain density were first put through a sieve with 500 μm-wide openings and then poured into the mold for sintering to attain 80% bulk porosity. All targets were heated from room to peak temperature in an oven under atmospheric pressure. Upon reaching peak temperature, each target was cooled naturally in the oven. We named the targets after their bulk porosities: fluffy94, fluffy87, and fluffy80, respectively. The typical target lengths and diameters were 130 and 62 mm, respectively, for fluffy94, 100 and 48 mm for fluffy87, and 130 and 62 mm for fluffy80. An example image of a target is shown in Fig. 1a.

We measured the targets' compressive strengths using a uniaxial compressive testing machine (EZ Graph, SHIMADZU Co.) at Kobe University, Japan. The samples, of size $20 \times 10\ \mathrm{mm}^2$ (length × diameter), were drilled from different depths of the targets, with their axes parallel to that of the cylindrical target. The core samples were placed in a load frame, which provided a record of the force applied and the displacement of the moving crosshead. The loading rate was 2 μm s^{-1}. Because of the targets' fluffiness, they could be easily compressed and their contact area with a top and a base plate spread until the stress eventually reached a maximum value and maintained this level. We considered the maximum force applied per unit area of the original cylinder to be the compressive strength of the targets. The compressive strength was higher for the samples at 0–50 mm and 0–25 mm from the top surface for fluffy94 and fluffy87, respectively probably because of the different thickness of the mold and the lid. The results are shown in Table 1, with a standard deviation of 4–6 measurements for different samples, which is much larger than the measurement errors.

Impact experiments were conducted using a two-stage light–gas gun at the Institute of Space and Astronautical Science (ISAS), Japan. The experimental configuration is illustrated in Fig. 1b. Targets were hung with a thread from the top of a target-support frame placed in a vacuum chamber under an ambient pressure of approximately 10 Pa. We positioned a high-speed video camera at a side window of the chamber and put a strobe light at the opposite side window to obtain shadowgraph images of projectile and target. The interval between frames was 2–8 μm. We used a flash X-ray system to observe the deceleration processes of the projectiles in non-transparent targets. Targets were illuminated by flash X-rays from two diagonal directions, and X-ray transmission images were recorded on two imaging plates. Controlling the timing of the X-ray exposure, we obtained two successive X-ray images with time intervals between 2 and 50 μs. Table 2 summarizes the experimental conditions. The projectiles were titanium, aluminum, and stainless-steel spheres and basalt cylinders. A cylindrical nylon sabot (Kawai et al., 2010) was used for projectile acceleration. The impact velocities ranged from 1.6 to 7.2 km s^{-1}.

The targets' track morphologies and the projectiles' final states were observed on transmission images taken by a micro-X-ray

Table 1
Sintering conditions and physical properties.

Target type	Peak temp. (°C)	Duration (h)	Compressive strength of stronger part[a] (MPa)	Compressive strength of weaker part [a] (MPa)	Porosity (%)
fluffy94	700	6	0.47 ± 0.13	0.27 ± 0.04	94.4 ± 0.2
fluffy87	800	6	1.43 ± 0.40	0.86 ± 0.10	86.8 ± 0.3
fluffy80	710	6	–[b]	–[b]	80.3 ± 0.9

[a] The compressive strength was higher for the samples at 0–50 mm and 0–25 mm from the top surface for fluffy94 and fluffy87, respectively (see the text).
[b] Compressive strength was not measured because of the target's brittleness.